Accurate Determination of Barrier Height and Kinetics for the F + H2O -> HF + OH Reaction

ARTICLE *in* THE JOURNAL OF PHYSICAL CHEMISTRY A · AUGUST 2013

Impact Factor: 2.69 · DOI: 10.1021/jp4069448 · Source: PubMed

5 AUTHORS, INCLUDING:

Thanh Lam Nguyen
University of Texas at Austin
72 PUBLICATIONS **1,382** CITATIONS
SEE PROFILE

Jun Li
Chongqing University
61 PUBLICATIONS **756** CITATIONS
SEE PROFILE

John F Stanton
University of Texas at El Paso
251 PUBLICATIONS **10,463** CITATIONS
SEE PROFILE

Hua Guo
University of New Mexico
382 PUBLICATIONS **7,533** CITATIONS
SEE PROFILE

THE JOURNAL OF PHYSICAL CHEMISTRY A

Article

pubs.acs.org/JPCA

Accurate Determination of Barrier Height and Kinetics for the F + H_2O → HF + OH Reaction

Thanh Lam Nguyen,[†,∥] Jun Li,[‡,∥] Richard Dawes,*[,§] John F. Stanton,*[,†] and Hua Guo*[,‡]

[†]Department of Chemistry and Biochemistry, The University of Texas at Austin, Austin, Texas, 78712, United States

[‡]Department of Chemistry and Chemical Biology, University of New Mexico, Albuquerque, New Mexico 87131, United States

[§]Department of Chemistry, Missouri University of Science and Technology, Rolla, Missouri 65409, United States

Supporting Information

ABSTRACT: The reaction energy and barrier height of the title reaction are investigated using two high-level *ab initio* protocols, namely Focal Point Analysis (FPA) and modified High Accuracy Extrapolated *Ab Initio* Thermochemistry (HEAT) methods. It is concluded from these calculations that despite some multireference character, dynamic electron correlation plays a dominant role near the reaction barrier. Thus, the coupled-cluster method with higher excitations than singles and doubles gives a better description than the multireference configuration interaction method for the barrier height. The FPA and HEAT classical barrier heights, including the spin−orbit and other corrections, are 1.919 and 2.007 kcal/mol, respectively. The rate constants and H/D kinetic isotope effect for the title reaction are determined by semiclassical transition-state theory based on the anharmonic potential energy surface near the saddle point, and the agreement with experiment is excellent. The rate constants are also computed using a quasi-classical trajectory method on a global potential energy surface scaled to the FPA barrier height and a similar level of agreement with experimental data is obtained.

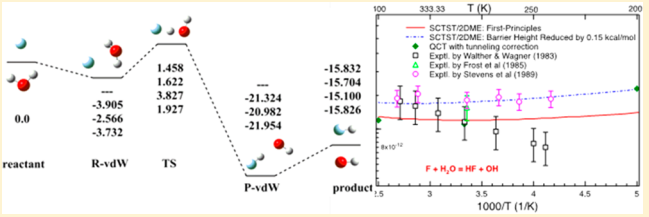

I. INTRODUCTION

The F + H_2O → HF + OH (ΔH^0_{rxn} = −17.63 ± 0.01 kcal/mol) reaction, which plays important roles in atmospheric[1] and astronomical chemistry,[2] has recently emerged as a prototype for studying atom−triatom reactions in the gas phase. Experimentally, the reaction is relatively straightforward to investigate because of its low barrier and the ease with which the products can be detected.[3−8] In addition, rate constants and kinetic isotope effects have been measured for this reaction.[9−11] Theoretically, this system is also attractive because the relatively small number (19) of electrons in the system makes it amenable to high-level electronic structure calculations,[12−16] and its six internal degrees of freedom allows exact quantum scattering studies.[15,17,18]

Despite these advances, there still exists an important controversy concerning the barrier height of the title reaction, which can significantly affect the reaction kinetics. In 2004, Deskevich et al.[12] obtained a barrier of ∼7 kcal/mol using a multireference configuration interaction (MRCI) method, but the transition-state geometry was only optimized at the complete active space self-consistent field (CASSCF) level. Previously in 2002, a barrier of merely 1.5 kcal/mol was reported by Ishikawa et al.,[19] using the Gaussian-2 second-order Møller−Plesset (G2MP2) method. More recently, a classical barrier height of 2.53 kcal/mol was reported by Li et al.[13] using the coupled-cluster singles and doubles and perturbative triples (CCSD(T)/cc-pV5Z) method, and it was reduced to 2.17 kcal/mol when the barrier correction from quadruple excitations was included. This number was close to 2.3 kcal/mol determined later at the CCSDT/cc-pVQZ level.[20] On the other hand, several of the current authors (J.L., R.D. and H.G.) found a barrier of 3.83 kcal/mol at the MRCI+Q/aug-cc-pVTZ level.[14] The best values at the single- and multireference levels differ by 1.66 kcal/mol.

It is quite surprising that such a large difference, which results in roughly an order of magnitude difference in the rate constant at low temperatures, exists for this relatively simple system. The argument for a multireference treatment was initially put forth by Deskevich et al.[12] based on the observation that there are several low-lying excited electronic states near the transition-state geometry. However, the calculated reaction cross section using our recent global potential energy surface (PES) based on MRCI calculations significantly underestimates the experimental results.[14] On the other hand, the barrier obtained using coupled-cluster methods such as CCSD(T) and CCSDT[13,20] are much closer to the activation energy derived from experimental rate constants.[9−11] It has been argued[13] that this reaction is similar to the F + H_2 → HF + H reaction, where the coupled-cluster methods were also significantly more accurate in computing the reaction barrier.[21] In addition, coupled-cluster methods have been found to give accurate barrier heights in other hydrogen abstraction reactions involving F.[22,23]

The different barrier heights for this reaction might stem from several possible causes. For example, both the MRCI and CC calculations have used relatively small basis sets. Other

Received: July 14, 2013
Revised: August 14, 2013
Published: August 15, 2013

   dx.doi.org/10.1021/jp4069448 | J. Phys. Chem. A 2013, 117, 8864−8872

corrections such as core−valence and relativistic effects were not taken into consideration. The CC methods are based on a single Slater determinant, and are therefore not optimal for non-dynamical electron correlation. On the other hand, the MRCI approach gives an imperfect description of the higher order excitations through the multireference analogue of the simple Davidson correction. To resolve this controversy, we present in this work extensive high-level ab initio studies on the barrier height and reaction energy for the title reaction using both the focal point analysis (FPA)[24,25] and the HEAT protocol.[26−28] The convergence behavior in FPA and its comparison with HEAT values reveals the key factors affecting the barrier height. In addition, the rate constants and H/D kinetic isotope effects are computed based on the anharmonic PES calculated with CCSD(T) near the saddle point using the semiclassical transition-state theory (SCTST) and a two-dimensional master equation technique.[29,30] Quasi-classical trajectory calculations of the rate constants have also been performed on a scaled PES, which reproduces the FPA barrier height. This publication is organized as follows. The next section (Section II) details the computational methods used in both the electronic structure and kinetic calculations. The ab initio and kinetic results are discussed in Sections III and IV. Section V summarizes.

II. THEORY

A. Focal Point Analysis. In FPA,[24,25] the structures for stationary points, including the transition state (TS), were first optimized using an all electron (AE) F12 UCCSD(T) method[31,32] with the cc-pCVTZ-F12 basis set,[33] which includes the core−electron correlation effect. The subsequent benchmark calculations were then carried out with the diffuse function augmented correlation consistent polarized valence *X* zeta basis sets, the aug-cc-pV*X*Z [*X* = 2(D), 3(T), 4(Q), 5, 6] basis sets.[34] For single-reference correlation methods, the reference electronic wave functions were determined by the single-configuration restricted, as well as unrestricted, open-shell Hartree−Fock (ROHF and UHF) methods. The coupled-cluster calculations up to CCSD(T) were performed using Molpro,[35] while the MRCC program[36] (interfaced to CFOUR[37] and Molpro) was employed in UCCSDT and UCCSDT(Q) calculations. The MRCC code only applies perturbative excitations to UHF references. So for UCCSDT, both ROHF and UHF can be used as the reference, while for UCCSDT(Q), only UHF is allowed. Thus, the reference electronic wave functions were determined at the level of ROHF up to UCCSDT, and UHF was used in UCCSDT(Q) calculations. Finally, we note that in this study FC denotes the use of the usual frozen-core approach for the electron correlation calculations, while AE indicates that all of the electrons are correlated.

Following the FPA approach,[24,25] the benchmark relative energies were determined at the optimized geometries considering:

(a) extrapolations to the complete basis set (CBS) limit using aug-cc-pV*X*Z (*X* = 5,6) basis sets;
(b) electron correlation beyond UCCSD(T) by performing UCCSDT/aug-cc-pVTZ, and UCCSDT(Q)/aug-cc-pVTZ calculations;
(c) core electron correlation effects as the difference between AE and FC UCCSD(T)/aug-cc-pCVQZ energies;
(d) scalar relativistic effects at the AE Douglas-Kroll-Hess UCCSD(T)/aug-cc-pCVQZ level (DKH2);
(e) experimental spin−orbital (SO) corrections only for the F and OH species.[38,39]

The energy contributions were then extrapolated to CBS limit as follows:

$$E_X^C = E_{CBS}^C + b/X^3 \quad (1)$$

where *C* denotes the energy contribution. The best two energies, i.e., X = 5 and 6 values, were used to get the CBS limiting for the energy increments. Finally, the energies were described as

$$E_{FPA} = E(\mathrm{UCCSDT(Q)} - \mathrm{FC})/\mathrm{CBS} + \Delta_{Core} + \Delta_{Rel} + \Delta_{SO} + \Delta_{DBOC} \quad (2)$$

where the Δ terms denote core correlation, relativistic, spin−orbit and diagonal Born−Oppenheimer corrections, respectively.

B. HEAT Calculations. All of the stable species, F, H_2O, OH, and HF, are part of the group of atoms and molecules used in previous systematic studies of the HEAT method.[26−28] Coupled-cluster calculations of the reaction energetics and barrier heights used a composite scheme virtually identical to the HEAT method.[26−28] Exceptions to the standard protocol designated as HEAT-345(Q)[28] employed in this work are: (1) the vibrational zero-point corrections to the energies were based on FC-CCSD(T) calculations using the ANO basis set,[40,41] which is an accurate[42] and cost-effective alternative to determining the zero-point energy at the AE-CCSD(T) level with the considerably larger cc-pVQZ basis set (that which is also used for determining the geometries used for the electronic energy calculations); and (2) experimental SO corrections were used for OH and F. Therefore, the HEAT protocol used in this work is a modification of the standard protocol,[26−28] and is named a modified HEAT-345(Q). All coupled-cluster calculations for HEAT were carried out with the CFOUR program system;[37] CCSDT(Q) calculations were done with the MRCC program.

In addition to the HEAT and FPA protocols, the systematic achievement of chemical accuracy through calculations including various basis set extrapolation procedures and the inclusion of high-order correlation and other corrections has been reported by others.[43,44]

C. Semiclassical Transition-State Theory. The general mechanism of the title reaction (formation of a reactant van der Waals complex (R-vdW) with subsequent abstraction), as presented in Figure 1, is ubiquitous in atmospheric and combustion chemistry. (The product van der Waals (P-vdW) complex is ignored here because of the large exothermicity of the title reaction.) Various chemical kinetic models used for the

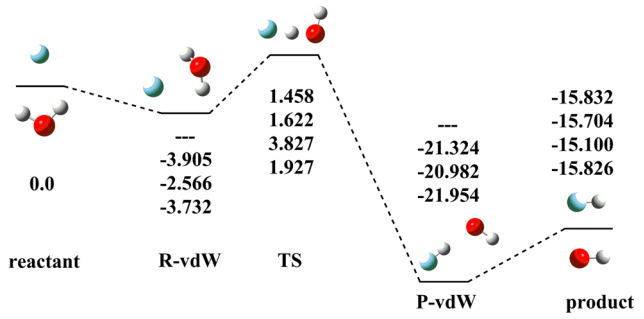

Figure 1. Schematic reaction path for the F + H_2O → HF + OH reaction, the numbers are in kcal/mol, the classical electronic enegies without SO corrections, relative to the reactant asymptote at various levels: FPA, HEAT, MRCI+Q/aug-cc-pVTZ,[14] and FC−CCSD(T)-F12b/aug-cc-pVTZ,[14] from top to bottom.

dx.doi.org/10.1021/jp4069448 | J. Phys. Chem. A 2013, 117, 8864−8872

treatments of such reactions have been detailed elsewhere.[45] Briefly, an analytical solution of the two-dimensional master equation (i.e., depending on both energy and overall rotation, designated hereafter as SCTST/2DME) for thermal rate constants under the low-pressure limit for a reaction scheme as shown in Figure 1 is given by eq 3.

$$k_{P=0}(T) = \frac{1}{h} \times \frac{Q^{\neq}_{\text{trans,elec}}}{Q_F Q_{H_2O}} \times \Sigma_{J=0}^{+\infty}(2J+1) \times \int_0^{+\infty} \frac{G_0^{\neq}(E,J) \times G_1^{\neq}(E,J)}{G_0^{\neq}(E,J) \times G_1^{\neq}(E,J)} \exp\left(-\frac{E}{k_B T}\right) dE \quad (3)$$

where h is Planck's constant, k_B is Boltzmann's constant, and Q_{H_2O} is the total partition function of H_2O. The electronic partition function of F, which has a $^2P_{3/2}$ ground state, is given by $Q_F^{\text{elec}} = 4 + 2\exp(-404\ \text{cm}^{-1}/k_B T)$. $Q^{\neq}_{\text{trans,elec}}$ is a product of translational and electronic partition functions corresponding to the reaction transition structure, TS. $G_1^{\neq}(E,J)$ is the rovibrational cumulative reaction probability (CRP) at each pair of (E,J) for TS. $G_0^{\neq}(E,J)$ is a rovibrational sum of states for the kinetic bottleneck for the R-vdW → F + H_2O step, which can be computed as a minimum of chemical reaction fluxes passing through the dividing surface using variational RRKM,[46,47] which define the transition state TS0. In this work, vibration and rotation are assumed to be separable, so $G(E,J)$ can be computed by convolution and expressed by

$$G(E,J) = \int_0^E G_{\text{vib}}(E - E_{\text{rot}}) \rho_{\text{rot}}(E_{\text{rot}})\, dE_{\text{rot}} \quad (4)$$

Here the vibrational CRP for TS, $G_1^{TS1}(E)$, is calculated using SCTST,[29,48] which includes fully coupled vibrations and multidimensional tunneling, while the vibrational sum of states for variational TS0 is calculated using the Beyer−Swinehart−Stein−Rabinovitch (BSSR) algorithm.[49,50] Rotational energy levels of a rigid symmetric top molecule are used for the transition states, given by $E_{\text{rot}} = \bar{B}J(J+1) + (A - \bar{B})K^2$ with $\bar{B} = (B \times C)^{1/2}$ and $-J \le K \le J$. Both the CRP and the rotational density of states are obtained by explicit state counting, using an energy bin size of 1 cm^{-1}, a maximum J of 200, and a ceiling energy of 5×10^4 cm^{-1} relative to the initial reactants. The latter two cutoffs are chosen to be high enough to ensure that all reaction rates computed in the temperature range from 100 to 2500 K are converged. Equation 3 is computed by simple summation using step sizes of 1 cm^{-1} and unity for E and J, respectively. It should be mentioned that the reaction path degeneracy of 2 (since R-vdW is of C_s symmetry and two hydrogens are identical) and 1 for the R-vdW → TS → HF + OH step and the R-vdW → variational TS0 → F + H_2O step, respectively, are also included into G_1 and G_0.

To check whether or not the rate of title reaction depends appreciably on pressure, thermal rate constants producing the final products (HF + OH) under the high-P limit are also computed using eq 5.

$$k_{P=\infty}(T) = k_0(T) \times \frac{k_1(T)}{k_{-0}(T) + k_1(T)} \quad (5)$$

where $k_0(T)$ and $k_{-0}(T)$ are thermal rate constants of the bimolecular association and redissociation reactions, F + H_2O ⇌ R-vdW, respectively, and $k_1(T)$ is a thermal rate constant of the unimolecular decomposition reaction of R-vdW → HF + OH. The ratio of $k_1(T)/[k_{-0}(T) + k_1(T)]$ corresponds to the fraction of R-vdW leading to the products under the condition of the thermal equilibrium. Because the prereactive complex stays in a shallow well and has a very short lifetime (on the order of a picosecond), the thermal stabilization of R-vdW can only occur under extreme conditions of very low temperature and extremely high pressure. As a result, eq 5 is highly unlikely to be a particularly useful model for applications to reactions of this sort that occur in the gas phase, such as in the atmosphere and combustion. In contrast, the thermal equilibrium is easy to be achieved for reactions in the solution.

Our calculated results (see Figure S1 in the Supporting Information (SI)) show that differences between eq 3 and eq 5 are negligibly small at moderate to high temperatures, but become more pronounced at low temperatures. At room temperature, the difference is only about 10%, likely within the uncertainty of a measurement. In the temperature range of 240 to 400 K where experimental data are available,[9−11] the calculated reaction rate constants depend slightly on pressure. As shown in previous work,[45] for the gas-phase reaction eq 3 provides more reliable values of $k(T)$ than eq 5 because all experiments[9−11] were done under conditions approximating the low-pressure limit. Unless noted otherwise, eq 3 will hereafter be used to calculate thermal rate constants of the title reaction.

D. QCT Calculations. 10^5 trajectories were calculated at temperatures T = 200, 300, 400, and 1000 K, respectively, using VENUS[51,52] based on a scaled PES (see below). The statistical errors are all smaller than 3%. The trajectories were initiated with a reactant separation of 7.0 Å, and terminated when products reached a separation of 15.0 Å, or when reactants are separated by 7.0 Å for nonreactive trajectories. The maximal impact parameter (b_{max}) was determined using small batches of trajectories with trial values. The other scattering parameters (impact parameter, vibrational phases, and spatial orientation of the initial reactants) were selected via a Monte Carlo approach. In particular, the angle variables for the H_2O normal modes were selected randomly and then converted to the initial coordinates and momenta along with fixed action variables.[51,52] During the propagation, the gradient of the PES was obtained numerically by a two-point central-difference algorithm. The propagation time step was selected to be 0.10 fs. Energy conservation of the trajectories was found to be excellent with the chosen time step. Almost all trajectories conserved energy to within a chosen criteria (0.04 kcal/mol), which confirms the smoothness of the PES. A few exceptionally long trajectories were halted if the propagation time reached a prespecified value (10.0 ps).

The translational, vibrational, and rotational degrees of freedom of the reactants are sampled at the specified temperature under the Boltzmann distribution rules. The rate constant was calculated as follows:

$$k_1 = Q_e \sqrt{\frac{8k_B T}{\pi \mu}}\, \pi b_{\text{max}}^2 \frac{N_r}{N_{\text{total}}} \quad (6)$$

in which N_r and N_{total} are the numbers of reactive and total trajectories and μ is the reduced mass for the reactant channel. The electronic partition function $Q_e = 2/Q_F^{\text{elec}}$ and Q_F^{elec} is the same in the SCTST calculations. Both hydrogen atoms are explicitly considered to be reactive in the QCT calculations, thus the symmetry factor 2 has been included.

dx.doi.org/10.1021/jp4069448 | J. Phys. Chem. A 2013, 117, 8864−8872

Table 1. Geometries of the Stationary Points for the F + H_2O → HF + OH Reaction on the Ground Electronic State in Internal Coordinates (Å for Lengths and ° for Angles)

species	method	R_{OH}	$R_{O\acute{H}}$	$R_{\acute{H}F}$	$\theta_{HO\acute{H}}$	$\theta_{O\acute{H}F}$	$\phi_{HO\acute{H}F}$
F+H_2O	AE-CCSD(T)-F12b/cc-pCVTZ-F12	0.9577	0.9577		104.52		
	2-state MRCI+Q_{rot}/aug-cc-pVTZ[14]	0.9602	0.9602		104.23		
	FC-CCSD(T)-F12b/aug-cc-pVTZ[14]	0.9586	0.9586		104.44		
	AE-CCSD(T)/cc-pVQZ	0.9562	0.9562		104.25		
R-vdW ($F^{\cdots}H_2O$)	AE-CCSD(T)-F12b/cc-pCVTZ-F12	0.9610	0.9610	2.2524	104.85	68.89	−84.68
	2-state MRCI+Q_{rot}/aug-cc-pVTZ[14]	0.9635	0.9635	2.4180	104.24	66.23	−90.38
	FC-CCSD(T)-F12b/aug-cc-pVTZ[14]	0.9620	0.9620	2.2475	104.77	69.12	−84.34
	AE-CCSD(T)/cc-pVQZ	0.9592	0.9592	2.2666	104.54	69.79	−83.85
TS	AE-CCSD(T)-F12b/cc-pCVTZ-F12	0.9671	1.0459	1.2866	103.46	125.39	68.29
	2-state MRCI+Q_{rot}/aug-cc-pVTZ[14]	0.9700	1.0370	1.3137	102.95	122.85	67.34
	FC-CCSD(T)-F12b/aug-cc-pVTZ[14]	0.9679	1.0421	1.2989	103.37	124.75	68.45
	AE-CCSD(T)/cc-pVQZ	0.9653	1.0431	1.2805	103.14	125.47	67.24
P-vdW ($HO^{\cdots}HF$)	AE-CCSD(T)-F12b/cc-pCVTZ-F12	0.9711	1.8150	0.9272	111.02	174.62	0.0
	2-state MRCI+Q_{rot}/aug-cc-pVTZ[14]	0.9752	1.8210	0.9286	110.46	174.88	0.0
	FC-CCSD(T)-F12b/aug-cc-pVTZ[14]	0.9721	1.8135	0.9279	111.00	174.55	0.0
	AE-CCSD(T)/cc-pVQZ	0.970	1.8143	0.9251	110.21	174.04	0.0
HO+HF	AE-CCSD(T)-F12b/cc-pCVTZ-F12	0.9695		0.9168			
	2-state MRCI+Q_{rot}/aug-cc-pVTZ[14]	0.9728		0.9202			
	FC-CCSD(T)-F12b/aug-cc-pVTZ[14]	0.9703		0.9176			
	AE-CCSD(T)/cc-pVQZ	0.9680		0.9152			
Ṕ-vdW ($OH^{\cdots}FH$)	AE-CCSD(T)-F12b/cc-pCVTZ-F12	0.9711	3.5715	0.9186	19.08	45.63	0.0
	2-state MRCI+Q_{rot}/aug-cc-pVTZ[14]	0.9749	3.4290	0.9207	23.64	54.72	0.0
	FC-CCSD(T)-F12b/aug-cc-pVTZ[14]	0.9721	3.4160	0.9196	23.67	54.32	0.0
	AE-CCSD(T)/cc-pVQZ	N/A	N/A	N/A	N/A	N/A	N/A

Table 2. Harmonic Frequencies (cm^{-1}) of the Reactants, Products, and TS for the F + H_2O → HF + OH Reaction

		harmonic frequency (cm^{-1})					
species	method	1	2	3	4	5	6
F+H_2O	AE-CCSD(T)-F12b/cc-pCVTZ-F12	3950.62	3840.12	1650.42			
	2-state MRCI+Q_{rot}/aug-cc-pVTZ[14]	3938.25	3835.59	1669.93			
	FC-CCSD(T)-F12b/aug-cc-pVTZ[14]	3943.65	3834.01	1648.26			
	AE-CCSD(T)/cc-pVQZ	3947.48	3835.04	1653.20			
TS	AE-CCSD(T)-F12b/cc-pCVTZ-F12	3781.29	2298.18	1375.47	561.38	398.05	1326.05*i*
	2-state MRCI+Q_{rot}/aug-cc-pVTZ[14]	3776.87	2452.24	1516.65	757.28	325.53	1891.98*i*
	FC-CCSD(T)-F12b/aug-cc-pVTZ[14]	3783.64	2357.70	1414.39	610.69	421.62	1221.37*i*
	AE-CCSD(T)/cc-pVQZ	3788.57	2281.77	1400.56	610.76	423.35	1466.77*i*
OH+HF	AE-CCSD(T)-F12b/cc-pCVTZ-F12	4144.90	3746.54				
	2-state MRCI+Q_{rot}/aug-cc-pVTZ[14]	4132.96	3722.02				
	FC-CCSD(T)-F12b/aug-cc-pVTZ[14]	4143.16	3741.28				
	AE-CCSD(T)/cc-pVQZ	4148.53	3739.07				

III. AB INITIO RESULTS

Table 1 compares the geometries of the stationary points in the title reaction at various high ab initio levels, including previous MRCI+Q/aug-cc-pVTZ and FC-CCSD(T)-F12b/aug-cc-pVTZ,[14] and current AE-CCSD(T)-F12b/cc-pCVTZ-F12 in FPA and AE-CCSD(T)/cc-pVQZ in HEAT. Generally speaking, the geometries from single-reference methods are in good agreement with each other, while MRCI+Q/aug-cc-pVTZ gives slightly different results. For instance, R-vdW has a larger $R_{H'F}$ at the MRCI+Q/aug-cc-pVTZ level; for TS, $R_{OH'}$ is shorter and $R_{H'F}$ is longer at the MRCI+Q/aug-cc-pVTZ level. The harmonic frequencies of the reactants, TS, and products are compared in Table 2.

Relative energies of various terms contributed to HEAT energies are tabulated in Table 3. The reaction energy computed with the modified HEAT-345(Q) method[28] used here is −17.62 kcal/mol (compared to −17.64 kcal/mol with the full HEAT-345(Q)). (This small discrepancy of 0.02 kcal/mol is due to a difference of ZPEs used in the standard (AE-CCSD(T)-ccpVQZ) and modified (FC−CCSD(T)/ANO) HEAT protocols.) Both of these are in rather startling—but certainly somewhat fortuitous—agreement with the value of −17.63 ± 0.01 kcal/mol that can be obtained from Ruscic's Active Thermochemical Tables (ATcT version 1.110),[53−55] and attest to the ability of HEAT-345(Q) to treat the thermochemistry of reactions involving small, relatively well-behaved molecules. The ZPE correction of −2.10 kcal/mol plays a key role to bring the HEAT value in line with the experiment, while the other corrections are small (ca. 0.19 kcal/mol) and make a minor contribution to the reaction enthalpy.

Without question, the most challenging stationary point treated here is the TS. For the barrier height, the unrestricted HF method provides a high value of 29.25 kcal/mol; electron

dx.doi.org/10.1021/jp4069448 | J. Phys. Chem. A 2013, 117, 8864−8872

Table 3. Relative Energies (kcal/mol) of Various Terms Contributed to the Modified HEAT Protocol[a]

species	δ[HF]	δ[CCSD(T)]	δ[CCSDT]	δ[CCSDT(Q)]	δ[REL]	δ[ZPE]	δ[DBOC]	δ[SO]	δ[HEAT]
F + H_2O	0.000	0.000	0.000	0.000	0.000	0.000	0.000	0.000	0.000
HF + HO	−9.474	−6.237	−0.042	−0.042	0.058	−2.104	0.033	0.186	−17.622 [−17.64][c]
TS	29.245	−26.767	−0.451	−0.376 [-0.494][b]	0.013	−1.280	0.076	0.385	0.845 [0.727][b]
R-vdW (F···H_2O)	8.987	−12.573	−0.281	−0.046	0.004	0.995	0.006	0.385	−2.525
P-vdW (FH···OH)	−13.458	−7.961	−0.041	−0.053	0.073	−0.284	0.115	0.385	−21.222

[a]Based on AE-CCSD(T)/cc-pVQZ optimized geometries. [b]The values in brackets are calculated with CCSDT(Q)/cc-pVTZ level of theory while the others are obtained with CCSDT(Q)/cc-pVDZ level of theory. [c]Taken from the standard HEAT-345(Q) protocol.[26−28]

correlation with the CCSD(T) method is found to be very important and reduces the barrier significantly by 26.77 kcal/mol. Higher-order correlation corrections to the barrier height are −0.451 and −0.494 kcal/mol from the CCSDT and CCSDT(Q) methods, respectively. Note that the latter value of −0.494 kcal/mol was obtained at CCSDT(Q)/cc-pVTZ level of theory, about 0.12 kcal/mol lower than that of −0.376 kcal/mol calculated with CCSDT(Q)/cc-pVDZ level of theory that used in the standard HEAT protocol. This is a surprising result because both of these higher-level correction effects regularly have opposite signs and they often cancel, according to our experience for stable species. This result indicates that the nature of wave function at the transition structure is complicated. The spin−orbit correction to the barrier height is 0.385 kcal/mol coming entirely from the experimental spin−orbit correction for F atom. In addition, the diagonal Born−Oppenheimer correction (DBOC) is small (0.076 kcal/mol) but not negligible. Finally, scalar relativistic effects are found to be very small (0.013 kcal/mol), as expected for the system with component of O, F, and H atoms. Taking all these corrections into account, we obtain 2.007 and 0.727 kcal/mol for the classical and vibrationally adiabatic barrier heights, respectively. The latter value will be used to obtain "first-principles" reaction rate constants using SCTST/2DME approach.

The uncertainty that should be attached to this value is certainly much greater than the average error in atomization energies for the HEAT-345(Q) method (0.08 kcal/mol with a maximum error of 0.18 kcal/mol), because of the aforementioned difficulty in treating the transition state. Apart from the large higher-order corrections to the barrier height, it also happens that the individual CCSD(T) to CCSDT and CCSDT(Q) corrections to the energy of the transition state itself (as opposed to the barrier height), which also tend to cancel for "normal" species, have the same sign in this example, and there is an individual quite large singles excitation amplitude of about 0.28. It should be pointed out, however, that spin contamination is not a problem with the UHF wave functions, as $\langle S^2 \rangle$ calculated at the SCF level is only about 0.77. Given the above, it would behoove us to associate a larger uncertainty (0.5 kcal/mol would be a conservative, but suitable, estimate) for the coupled-cluster-based barrier height computed here.

The benchmark FPA results for the reaction energy and the classical barrier height are given in Tables 4 and 5, respectively, using the geometries at the level of AE-CCSD(T)-F12b/cc-pCVTZ-F12. As shown, electron correlation plays an important role in the accurate determination of the energies. One has to employ triples (at least perturbatively) such as with the CCSD(T) method to achieve reasonable convergence for the reaction energy; the post-CCSD(T) correlation contributions are only −0.044 and 0.007 kcal/mol, respectively, both of which are negligible compared to the reaction energies of −15.932 kcal/mol at the FC-UCCSDT(Q)/CBS level, −14.940 kcal/mol at the AE-MRCI+Q/aug-cc-pwCV5Z level (see SI), or −15.826 kcal/mol at the FC-CCSD(T)-F12b/aug-cc-pVTZ level.[14] The basis set completeness also affects the reaction energy to some extent. The reaction energy from FPA (Table 4) follows −14.991, −15.752, and −15.978 kcal/mol, respectively, for X = D, T, and Q in the basis series of aug-cc-pVXZ. The sum of the core electron correlation (Δ_{core}) and the scalar relativistic effect (Δ_{Rel}) is 0.100 kcal/mol. The SO effect from F and OH is significant, since it changes the reaction energy by 0.186 kcal/mol. For the DBOC correction, we have used the value computed in HEAT (0.033 kcal/mol). With all contributions taken into account, the classical reaction energy employing the FPA method is benchmarked to be −15.613 kcal/mol, which becomes −17.827 kcal/mol after ZPE corrections from AE-CCSD(T)-F12b/cc-pCVTZ-F12 were considered. It agrees well with the HEAT-345(Q) value of −17.64 kcal/mol (see SI), which is within the narrow error bars of the ATcT value of −17.63 ± 0.01 kcal/mol.

For the classical barrier height, as shown in Table 5, the post-CCSD(T) correlation contributions are relatively large for this low barrier: δ[CCSDT] = −0.288 kcal/mol, and δ[CCSDT(Q)] = −0.494 kcal/mol. This is not seen in the reaction energy. In fact the barrier at the restricted open-shell Hartree−Fock level is 39.0 kcal/mol and drops enormously at each correlation level. So for the barrier height, especially for the low barrier in this system, inclusion of high-order correlation is essential. At the level of FC-UCCSDT(Q)/CBS, the classical barrier height is 1.413 kcal/mol, compared to 3.827 kcal/mol at the MRCI+Q/aug-cc-pVTZ level and 1.927 kcal/mol at the FC-CCSD(T)-F12b/aug-cc-pVTZ level.[14] The basis effect is even more significant since the barrier height changes significantly with increasing basis set size until it is finally apparently converged between aug-cc-pV5Z and aug-cc-pV6Z. The sum of the core electron correlation (Δ_{core}) and the scalar relativistic effect (Δ_{Rel}) is 0.045 kcal/mol. The SO effect for the barrier height is significant, since it increases the barrier height by 0.385 kcal/mol. Similarly, the DBOC correction of 0.076 kcal/mol is adapted from the HEAT calculation. Finally, the barrier height is benchmarked to be 1.919 kcal/mol using FPA, or 2.007 kcal/mol using HEAT. The barriers calculated in this work are much lower than the 3.827 kcal/mol value in the MRCI+Q/aug-cc-pVTZ calculations,[14] but close to the 2.3 kcal/mol value at the CCSDT/cc-pVQZ level by Li et al.,[20] and 1.927 kcal/mol at the FC-CCSD(T)-F12b/aug-cc-pVTZ level[14] (the latter three values are free of SO corrections, which make them even larger).

It is interesting to note that the observations in the current system are quite similar to those in the F + CH_4 system.[56] Both systems have early barriers and the barriers are quite low. In particular, the HF method was found to grossly overestimate the barrier height for the F + CH_4 reaction, underscoring the important role played by dynamical electron correlation. In addition, the contributions beyond CCSD(T) in F + H_2O, defined as the

Table 4. FPA of the Classical Reaction Exothermicity (ΔE in kcal/mol) of the F + H_2O → HF + OH Reaction[a]

	ΔE[HF]	δ[MP2]	δ[CCSD]	δ[CCSD(T)]	δ[CCSDT]	δ[CCSDT(Q)]	ΔE
aug-cc-pVDZ	−9.003	−6.555	+0.638	+0.013	−0.066	−0.018	−14.991
aug-cc-pVTZ	−9.461	−6.981	+0.996	−0.257	−0.056	+0.007	−15.752
aug-cc-pVQZ	−9.404	−7.280	+1.041	−0.298	−0.044	[+0.007]	−15.978
aug-cc-pV5Z	−9.373	−7.265	+1.063	−0.308	[-0.044]	[+0.007]	−15.920
aug-cc-pV6Z	−9.370	−7.281	+1.076	−0.313	[-0.044]	[+0.007]	−15.925
CBS[b]	−9.366	−7.303	+1.094	−0.320	−0.044	0.007	**-15.932**

ΔE (FPA) = ΔE (FC-UCCSDT(Q)) + Δ_{Core} + Δ_{Rel} + Δ_{SO} + Δ_{DBOC} = −15.932 + 0.045 + 0.055 + 0.186 + 0.033 = **−15.613**. After ZPE corrections at UCCSD(T)-F12b-AE/cc-pCVTZ-F12, it becomes **−17.827** kcal/mol ATcT: **−17.63 ± 0.01** kcal/mol

[a]The results correspond to the structures optimized at the AE-CCSD(T)-F12b/cc-pCVTZ-F12 level of theory. The symbol δ denotes the increments in ΔE with respect to the preceding level of theory. Brackets signify assumed, nonextrapolated, increments from smaller basis set results, as the calculations at that level are not practical. The final FPA results, **−15.613** and **−15.932**, are with and without small corrections (core, relativistic, SO, and DBOC). [b]The CBS energy and energy increment were calculated using two-parameter extrapolation formulas given in eq 1. Only the best two energies were included in the extrapolations.

Table 5. FPA of the Classical Reaction Barrier (E^* in kcal/mol) of the F + H_2O → HF + OH Reaction[a]

	E^*[HF]	δ[MP2]	δ[CCSD]	δ[CCSD(T)]	δ[CCSDT]	δ[CCSDT(Q)]	E^*
aug-cc-pVDZ	37.906	−24.602	−6.510	−3.691	−0.899	−0.312	1.892
aug-cc-pVTZ	38.559	−25.564	−5.577	−5.193	−0.288	−0.494[b]	1.443
aug-cc-pVQZ	38.866	−26.060	−5.204	−5.507	[−0.288]	[−0.494]	1.313
aug-cc-pV5Z	38.973	−26.070	−5.062	−5.613	[−0.288]	[−0.494]	1.446
aug-cc-pV6Z	38.986	−26.120	−5.003	−5.649	[−0.288]	[−0.494]	1.432
CBS	39.004	−26.189	−4.922	−5.698	−0.288	−0.494	**1.413**

E^*(FPA) = E^*(FC-UCCSDT(Q)) + Δ_{Core} + Δ_{Rel} + Δ_{SO} + Δ_{DBOC} = **1.413** + 0.037 + 0.008 + 0.385 + 0.076 = **1.919**

[a]See the footnote of Table 4 for the notations. [b]Obtained with CCSDT(Q)/cc-pVTZ level of theory.

sum of δ[CCSDT] and δ[CCSDT(Q)], are −0.084/−0.037 and −0.945/−0.728 kcal/mol for the reaction energy and barrier at the levels of HEAT/FPA. These values can be compared with those for F + CH_4 (−0.076 and −0.244 kcal/mol using FPA). Apparently, the classical barriers in both reactions are significantly affected by the higher order excitations, but the effects on reaction energies are small.

Multireference calculations were performed for the ground state and lowest four excited states as reported by Deskevich et al.[12] The leading reference coefficient at the transition structure is 0.91. This indicates that the TS region is only borderline for requiring a multiconfigurational description. In CASSCF calculations at the TS, the first excited state of F + H_2O is about 25 kcal/mol above the ground state, and no significant mixing is observed when multiple MRCI states are computed. This is qualitatively different from Cl + H_2O the leading reference coefficient is only 0.82, and the excited state is much closer (13 kcal/mol).[57] For F + H_2O, given the dramatic effect of higher correlation on the barrier height, the most reliable estimate of the barrier height clearly requires the highest possible correlation treatment. Using the VQZ-F12 basis (see Table S11), the barrier height drops from 21.93 kcal/mol at the full-valence CASSCF level, to 8.01 kcal/mol at the explicitly correlated MRCI-F12 level, to 4.81 kcal/mol with addition of the Davidson correction. This is still far from the values around 2 kcal/mol discussed above for the coupled-cluster based methods including the highest levels of correlation. The unusually large effect of the Davidson correction is a strong indication of the importance of high-order correlation. This presents a difficult situation when a global PES is required and multiconfigurational and multistate treatments may be required in some regions (yet higher-excitations are prohibitively expensive for multireference methods).

IV. SCALED PES

At the level of two-state MRCI+Q_{rot}-DW-5-CASSCF(15e, 10o)/aug-cc-pVTZ, the classical barrier and the reaction energy for the reaction F + H_2O → HF + OH are 3.83 and −15.10 kcal/mol, respectively.[14] The reaction exothermicity is −17.81 kcal/mol at 0 K, while it becomes −15.78 kcal/mol if the SO corrections and ZPEs corrections of the reactants and products are removed.[15] With the FPA method without the small corrections as defined in eq 2, they are 1.41 and −15.93 kcal/mol, respectively, which can be compared to 1.74 and −15.70 kcal/mol at the HEAT-345(Q) values. It is clear that our original global PES for the title reaction based on the MRCI+Q_{rot} approach[14,15] overestimates the barrier about 2.1−2.4 kcal/mol, while the reaction energy was underestimated by about 0.8 kcal/mol. Following the idea of Brown and Truhlar[58] and Ramachandran and Peterson,[59] a simple global external correlation energy scaling procedure was employed to recover the accurate barrier and reaction energy. Particularly, a uniform parameter near unity is used to scale the external correlation energy based on the known information while retaining the qualitative shape of the global PES and not introducing any discontinuities. The external correlation energy is defined as the difference between the MRCI+Q_{rot} energy and the DW-CAS energy, namely,

$$E_{corr} = E_{MRCI+Q} - E_{DW\text{-}CAS} \quad (7)$$

The scaled total energy is then the sum of the DW-CAS energy plus the external correlation energy scaled by a constant factor, λ,

$$E_{scaled} = E_{DW\text{-}CAS} + \lambda E_{corr} \quad (8)$$

In the limit of $\lambda = 0$, no external correlation energy is recovered, whereas for $\lambda = 1$, the full MRCI+Q_{rot} correlation energy is obtained. Allowing λ to be greater than one permits recovery of additional correlation energy, in effect, approximating an increase in active space. The value of λ is empirically chosen to reproduce

dx.doi.org/10.1021/jp4069448 | J. Phys. Chem. A 2013, 117, 8864−8872

some known accurate data, such as barrier or reaction energy, namely,

$$\Delta E_{\text{scaled}} = \Delta E_{\text{exact}} \quad (9)$$

In this work, the classical barrier, 1.413 kcal/mol, at the level of FPA scheme was used to define the parameter λ, 1.135. The reaction energy was then scaled to be −16.23 kcal/mol, comparable to the −15.93 and −15.70 kcal/mol, respectively, at the FPA and HEAT levels without SO and other small corrections. The rate constant calculations discussed below show that the experimental results can be reproduced using eq 3 when the HEAT barrier height was reduced by 0.15 to 1.857 kcal/mol. In other words, the newly scaled PES is experimentally accurate in the barrier. Figure 2 shows a contour plot of the newly scaled

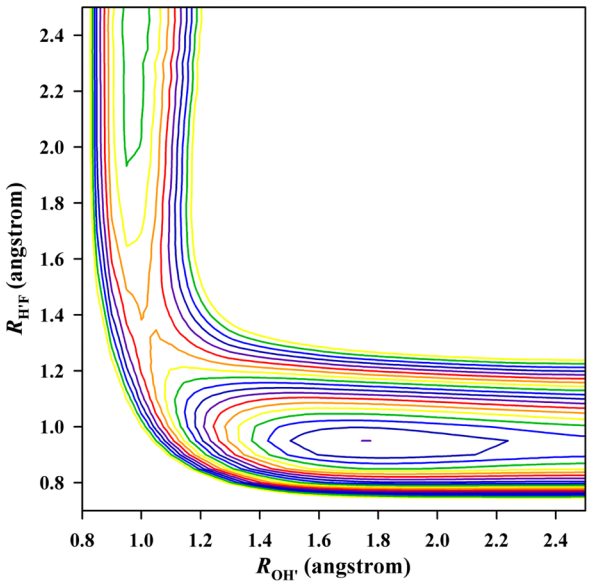

Figure 2. Contour plot for the newly scaled PES along the H′−F and O−H′ distances with all other internal coordinates optimized. Energies are in the range of 0−36 kcal/mol relative to the global minimum, P-vdW, and the interval is 2 kcal/mol.

PES with SO corrections[15] representing the two bond lengths involved in the title reaction while all other degrees of freedom are optimized. We intend to carry out dynamic calculation on this new PES in the near future.

V. RATE CONSTANTS

The calculated thermal rates for F + H_2O and D_2O reactions in the temperature range of 200 to 400 K using the SCTST/2DME approach are displayed in Figures 3 and 4 (also see Figures S1−S3). Available experimental data[9−11] is also included for the purpose of comparison. Inspection of Figures 3 and 4 reveals that our first-principles $k(T)$ with the ab initio barrier of 2.007 kcal/mol are slightly below the measurements by less than 30% in a temperature range of 240 to 370 K. Reducing the ab initio barrier height by 0.15 kcal/mol (as is consistent with the expected error of the HEAT method for the barrier height, which is ≤0.5 kcal/mol), the calculated $k(T)$ are certainly in line with all experimental results[11] for both F + H_2O and D_2O reactions. Possible effects of basis sets used in the ro-vibrational and anharmonic calculations on calculated $k(T)$ were investigated and found to be small (see Figure S4). Figure 3 also shows the calculated thermal rates for F + H_2O reaction show a (very) slight

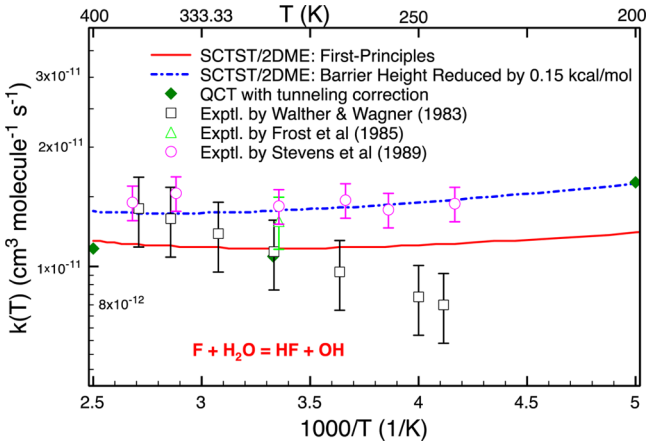

Figure 3. Calculated thermal rate constants as a function of temperature for F + H_2O reaction. Available experimental data were included for comparison.

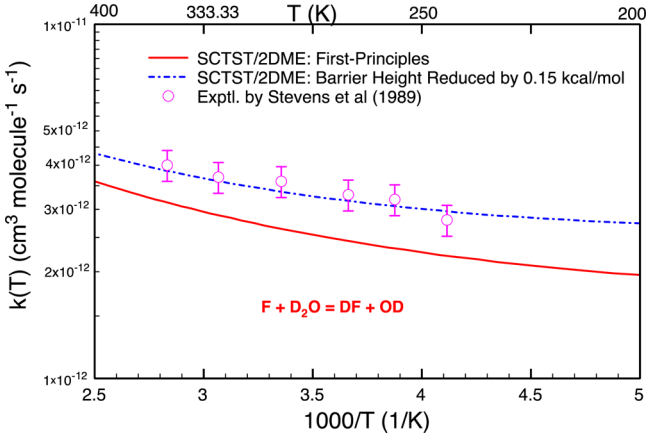

Figure 4. Calculated thermal rate constants as a function of temperature for F + D_2O reaction. Available experimental data were included for comparison.

negative temperature dependence in the range of 200 to 400 K, whereas those for F + D_2O reaction depend positively on temperature (see Figure 4), as is consistent with one experiment,[11] but differs somewhat from another measurement.[9] This different behavior is mainly due to coupled effects of zero-point vibrational energy and tunneling. Because of the low barrier height, tunneling correction is found to be small (see Figure S5). For example, the tunneling correction is 3.5 at 200 K, reduces to about 2.0 at 300K, and becomes 1.5 at 400 K. We also calculated the kinetic isotopic effect (KIE) of H_2O/D_2O. At room temperature, we obtained a KIE value of 4.17 using the ab initio barrier height and 4.08 with the adjusted barrier. They both are in agreement with 3.95 ± 0.3 derived from the experimental work of Stevens et al.[11]

The thermal rate constants have also been computed using the QCT method on the scaled PES with SO corrections at temperatures T = 200, 300, 400, and 1000 K. The results are also included in Figure 3 (also see Figure S3). Since the tunneling effect is not taken into account in the QCT calculations, the tunneling factors calculated above—3.5 at 200 K, 2.0 at 300 K, 1.5 at 400 K, 1.1 at 1000 K—were adopted in the QCT rate constants. It is clear that the QCT rate constants on the scaled PES are in good agreement (within 20%) with the experimental

dx.doi.org/10.1021/jp4069448 | J. Phys. Chem. A 2013, 117, 8864−8872

and SCTST results, and also show a slight negative temperature dependence in the range of 200 to 400 K.

V. SUMMARY

In this publication, various high-level ab initio methods were used to give an accurate determination of the barrier height and reaction energy for the F + H_2O reaction. Based on these extensive benchmark electronic structure calculations and subsequent kinetics investigations, it is concluded that

(i) Despite some multireference character, the MRCI treatment of the barrier height including singles and doubles excitations is not sufficiently accurate for the barrier height. The higher-order corrections beyond CCSD(T), δ[CCSDT] = −0.288, and δ[CCSDT(Q)] = −0.494 kcal/mol, significantly lower the barrier. For the reaction energy, on the other hand, the contributions from post-CCSD(T) computations are much smaller.

(ii) The barrier height for the title reaction is benchmarked to be 1.919 and 2.007 kcal/mol using the FPA and HEAT methods. The rate constants based on the former value are found to agree with experimental results. The H/D kinetics isotope effect is accurately reproduced. A negative temperature dependence of the rate constants in the range of 200−400K apparently results from tunneling. The R-vdW complex plays important roles in the chemical kinetics and dynamics.

(iii) The newly scaled PES based on the FPA barrier height is shown to reproduce the experimental and SCTST/2DME rate constants. This PES is expected to be more reliable for describing both the kinetic and dynamic attributes for the title reaction.

■ ASSOCIATED CONTENT

Supporting Information

Optimized geometries, rovibrational parameters, anharmonic constants, energies for various species, and calculated thermal rate constants in the reaction of F atom with water are given. This material is available free of charge via the Internet at http://pubs.acs.org.

■ AUTHOR INFORMATION

Corresponding Authors

*E-mail: dawesr@mst.edu.
*E-mail: jfstanton@gmail.com.
*E-mail: hguo@unm.edu.

Author Contributions

‖Equal contributions.

Notes

The authors declare no competing financial interest.

■ ACKNOWLEDGMENTS

This work was founded by the U.S. Department of Energy (DE-FG02-05ER15694 to HG) and the NSF (CHE-1300945 to RD). J.F.S. and T.L.N. are supported by the Robert A. Welch Foundation (Grant F-1283) and the Department of Energy, Office of Basic Energy Sciences (Contract Number DE-FG02-07ER15884). H.G. thanks Yaoming Xie and Fritz Schaefer for communicating their results before publication and for discussions. We would like to thank John R. Barker for helpful discussions.

■ REFERENCES

(1) Ricaud, P.; Lefevre, F., Fluorine in the Atmosphere. In *Fluorine and the Environment*, Tressaud, A., Ed. Elsevier: Amsterdam, 2006.

(2) Neufeld, D. A.; Zmuidzinas, J.; Schilke, P.; Phillips, T. G. Discovery of Interstellar Hydrogen Fluoride. *Astrophys. J.* **1997**, *488*, L141−145.

(3) Duewer, W. H.; Setser, D. W. Infrared Chemiluminescence and Energy Partitioning from Reactions of Fluorine Atoms with Hydrides of Carbon, Silicon, Oxygen, Sulfur, Nitrogen, and Phosphorus. *J. Chem. Phys.* **1973**, *58*, 2310−2320.

(4) Wickramaaratchi, M. A.; Setser, D. W.; Hildebrandt, H.; Korbitzer, B.; Heydtmann, H. Evaluation of HF Product Distributions Deduced from Infrared Chemiluminescence II. F Atom Reactions. *Chem. Phys.* **1985**, *94*, 109−129.

(5) Agrawalla, B. S.; Setser, D. W. Infrared Chemiluminescence and Laser-Induced Fluorescence Studies of Energy Disposal by Reactions of F-Atoms and Cl-Atoms with H_2S (D_2s), H_2Se, H_2O (D_2O), and CH_3OH. *J. Phys. Chem.* **1986**, *90*, 2450−2462.

(6) Ziemkiewicz, M.; Wojcik, M.; Nesbitt, D. J. Direct Evidence for Non-Adiabatic Dynamics in Atom+Polyatom Reactions: Crossed-Jet Laser Studies of F + D_2O → DF + OD. *J. Chem. Phys.* **2005**, *123*, 224307.

(7) Zolot, A. M.; Nesbitt, D. J. Crossed Jet Reactive Scattering Dynamics of F + H_2O → HF(v,j) + OH(v,j): HF(v,j) Product Quantum State Distributions under Single-Collision Conditions. *J. Chem. Phys.* **2008**, *129*, 184305.

(8) Ziemkiewicz, M.; Nesbitt, D. J. Nonadiabatic Reactive Scattering in Atom+Triatom Systems: Nascent Rovibronic Distributions in F + H_2O → HF + OH. *J. Chem. Phys.* **2009**, *131*, 054309.

(9) Walther, C. D.; Wagner, H. G. On the Reactions of F Atoms with H_2O, H_2O_2 and NH_3. *Ber. Bunsen-Ges. Phys. Chem.* **1983**, *87*, 403−409.

(10) Frost, R. J.; Green, D. S.; Osborn, M. K.; Smith, I. W. M. Time-Resolved Vibrational Chemiluminescence - Rate Constants for the Reactions of F-Atoms with H_2O and HCN, and for the Relaxation of HF (v = 1) by H_2O and HCN. *Int. J. Chem. Kinet.* **1986**, *18*, 885−898.

(11) Stevens, P. S.; Brune, W. H.; Anderson, J. G. Kinetic and Mechanistic Investigations of F + H_2O/D_2O and F + H_2/D_2 over the Temperature Range 240−373 K. *J. Phys. Chem.* **1989**, *93*, 4068.

(12) Deskevich, M. P.; Nesbitt, D. J.; Werner, H.-J. Dynamically Weighted Multiconfiguration Self-Consistent Field: Multistate Calculations for F + H_2O → HF + OH Reaction Paths. *J. Chem. Phys.* **2004**, *120*, 7281−7289.

(13) Li, G.; Zhou, L.; Li, Q.-S.; Xie, Y.; Schaefer, H. F., III. The Entrance Complex, Transition Sate, and Exit Complex for the F + H_2O → Hf + OH Reaction. Definitive Predictions. Comparison with Popular Density Functional Methods. *Phys. Chem. Chem. Phys.* **2012**, *14*, 10891−10895.

(14) Li, J.; Dawes, R.; Guo, H. An Ab Initio Based Full-Dimensional Global Potential Energy Surface for $FH_2O(X^2a')$ and Dynamics for the F + H_2O → HF + HO Reaction. *J. Chem. Phys.* **2012**, *137*, 094304.

(15) Li, J.; Jiang, B.; Guo, H. Spin-Orbit Corrected Full-Dimensional Potential Energy Surfaces for the Two Lowest-Lying Electronic States of FH_2O and Dynamics for the F + H_2O → HF + OH Reaction. *J. Chem. Phys.* **2013**, *138*, 074309.

(16) Li, J.; Li, Y.; Guo, H. Communication. Covalent Nature of the X···H_2O (X = F, Cl, Br) Interactions. *J. Chem. Phys.* **2013**, *138*, 141102.

(17) Li, J.; Jiang, B.; Guo, H. Enhancement of Bimolecular Reactivity by a Pre-Reaction van der Waals Complex: The Case of F + H_2O → HF + HO. *Chem. Sci.* **2013**, *4*, 629−632.

(18) Li, J.; Jiang, B.; Guo, H. Vibrational Excitations of Reactant Are More Effective Than Translational Energy in Promoting an Early-Barrier Reaction F + H_2O → HF + OH. *J. Am. Chem. Soc.* **2013**, *135*, 982−985.

(19) Ishikawa, Y.; Nakajima, T.; Yanai, T.; Hirao, K. Ab Initio Direct Molecular Dynamics Study of the Fragmentation of F(H_2O) Complex Generated by Photodetachment of F^-(H_2O) Anion Complex. *Chem. Phys. Lett.* **2002**, *363*, 458.

(20) Li, G.; Li, Q.-S.; Xie, Y.; Schaefer, H. F., III. The F + $(H_2O)_2$ Reaction: The Second Water Removes the Barrier. *J. Phys. Chem. A* **2013**, in press.

(21) Werner, H. J.; Kallay, M.; Gauss, J. The Barrier Height of the F +H_2 Reaction Revisited: Coupled-Cluster and Multireference Configuration-Interaction Benchmark Calculations. *J. Chem. Phys.* **2008**, *128*, 034305.

(22) Czakó, G.; Bowman, J. M. Quasiclassical Trajectory Calculations of Correlated Product Distributions for the F+CHD_3(v_1 = 0,1) Reactions Using an Ab Initio Potential Energy Surface. *J. Chem. Phys.* **2009**, *131*, 244302.
(23) Li, A.; Guo, H.; Sun, Z. G.; Kłos, J.; Alexander, M. H. State-to-State Quantum Dynamics of the F + HCl ($v_i = 0, j_i = 0$) → HF(v_f, j_f) + Cl Reaction on the Ground State Potential Energy Surface. *Phys. Chem. Chem. Phys.* **2013**, *15*, 15347−15355.
(24) Allen, W. D.; East, L. L.; Császár, A. G. In *Structures and Conformations of Non-rigid Molecules*, Laane, J.; Dakkouri, M.; van der Veken, B.; Oberhammer, H., Eds.; Kluwer: Dordrecht, The Netherlands, 1993.
(25) Császár, A. G.; Allen, W. D.; Schaefer, H. F., III. In Pursuit of the Ab Initio Limit for Conformational Energy Prototypes. *J. Chem. Phys.* **1998**, *108*, 9751−9764.
(26) Tajti, A.; Szalay, P.; Császár, A. G.; Kállay, M.; Gauss, J.; Valeev, E. F.; Flowers, B. A.; Vázquez, J.; Stanton, J. F. Heat: High Accuracy Extrapolated Ab Initio Thermochemistry. *J. Chem. Phys.* **2004**, *121*, 11599.
(27) Bomble, Y. J.; Vázquez, J.; Kállay, M.; Michauk, C.; Szalay, P. G.; Császár, A. G.; Gauss, J.; Stanton, J. F. High-Accuracy Extrapolated Ab Initio Thermochemistry. II. Minor Improvements to the Protocol and a Vital Simplification. *J. Chem. Phys.* **2006**, *125*, 064108.
(28) Harding, M. E.; Vázquez, J.; Ruscic, B.; Wilson, A. K.; Gauss, J.; Stanton, J. F. High-Accuracy Extrapolated Ab Initio Thermochemistry. III. Additional Improvements and Overview. *J. Chem. Phys.* **2008**, *128*, 114111.
(29) Nguyen, T. L.; Stanton, J. F.; Barker, J. R. A Practical Implementation of Semi-Classical Transition State Theory for Polyatomics. *Chem. Phys. Lett.* **2010**, *499*, 9−15.
(30) Nguyen, T. L.; Xue, B. C.; Weston, R. E., Jr.; Barker, J. R.; Stanton, J. F. Reaction of HO with CO: Tunneling Is Indeed Important. *J. Phys. Chem. Lett.* **2012**, *3*, 1549−1553.
(31) Adler, T. B.; Knizia, G.; Werner, H.-J. A Simple and Efficient CCSD(T)-F12 Approximation. *J. Chem. Phys.* **2007**, *127*, 221106.
(32) Knizia, G.; Adler, T. B.; Werner, H.-J. Simplified CCSD(T)-F12 Methods: Theory and Benchmarks. *J. Chem. Phys.* **2009**, *130*, 054104.
(33) Hill, J. G.; Mazumder, S.; Peterson, K. A. Correlation Consistent Basis Sets for Molecular Core-Valence Effects with Explicitly Correlated Wave Functions: The Atoms B−Ne and Al−Ar. *J. Chem. Phys.* **2010**, *132*, 054108.
(34) Kendall, R. A.; Dunning, T. H.; Harrison, R. J. Electron Affinities of the First-Row Atoms Revisited. Systematic Basis Sets and Wave Functions. *J. Chem. Phys.* **1992**, *96*, 6796−6806.
(35) *Molpro, version 2012.1, A Package of Ab Initio Programs*; Werner, H.-J.; Knowles, P. J.; Knizia, G.; Manby, F. R.; Schütz, M.; et al. See http://www.molpro.net.
(36) Kallay, M. MRCC, A Quantum Chemical Program Suite Written by M. Kállay, Rolik, Z.; I. Ladjánszki, Szegedy, L.; B. Ladóczki, Csontos, J.; B. Kornis. See also Kállay, M.; Rolik, Z. *J. Chem. Phys.* **2011**, *135*, 104111. as well as www.mrcc.hu.
(37) Stanton, J. F. *CFOUR, Coupled-Cluster Techniques for Computational Chemistry, a Quantum-Chemical Program Package by* Stanton, J.F.; Gauss, J.; Harding, M.E.; Szalay, P.G.; with contributions from Auer, A.A.; Bartlett, R.J.; Benedikt, U.; Berger, C.; Bernholdt, D.E.; Bomble, Y.J.; Cheng, L.; Christiansen, O.; Heckert, M.; Heun, O.; Huber, C.; Jagau, T.-C.; Jonsson, D.; J. Jusélius, Klein, K.; Lauderdale, W.J.; Matthews, D.A.; Metzroth, T.; L. A. Mück, D. P. O'neill, Price, D.R.; Prochnow, E.; Puzzarini, C.; Ruud, K.; Schiffmann, F.; Schwalbach, W.; Stopkowicz, S.; Tajti, A.; J. Vázquez, Wang, F.; Watts, J.D.; and the Integral Packages Molecule (J. Almlöf and P.R. Taylor), Props (P.R. Taylor), Abacus (T. Helgaker, H.J. Aa. Jensen, P. Jørgensen, and J. Olsen), and ECP Routines by A. V. Mitin and C. Van Wüllen. For the current version, see http://www.cfour.de.
(38) Moore, C. E., *Atomic Energy Levels (NSRDS-NBS 35)*; Office of Standard Reference Data, National Bureau of Standards: Washington DC, 1971.
(39) Huber, K. P.; Herzberg, G.; *Molecular Spectra and Molecular Structure, IV, Constants of Diatomic Molecules*; van Norstrand: Princeton, NJ, 1979.
(40) Almlof, J.; Taylor, P. R. General Constraction of Gaussian-Basis Sets. 1. Atomic Natural Orbitals for 1st-Row and 2nd-Row Atoms. *J. Chem. Phys.* **1987**, *86*, 4070−4077.
(41) Almlof, J.; Taylor, P. R. General Constraction of Gaussian-Basis Sets. 2. Atomic Natural Orbitals and the Calculation of Atomic and Molecular-Properties. *J. Chem. Phys.* **1990**, *92*, 551−560.
(42) McCaslin, L.; Stanton, J. F. Calculation of Fundamental Frequencies for Small Polyatomic Molecules: a Comparison between Correlation Consistent and Atomic Natural Orbital Basis Sets. *Mol. Phys.* **2013**, *111*, 1492−1496.
(43) Feller, D.; Peterson, K. A.; Crawford, T. D. Sources of Error in Electronic Structure Calculations on Small Chemical Systems. *J. Chem. Phys.* **2006**, *124*, 054107.
(44) Feller, D.; Peterson, K. A. Probing the Limits of Accuracy in Electronic Structure Calculations: Is Theory Capable of Results Uniformly Better Than Chemical Accuracy? *J. Chem. Phys.* **2007**, *126*, 114105.
(45) Nguyen, T. L.; Stanton, J. F. Ab Initio Thermal Rate Calculations of HO + HO = O(^{3}P) + H_2O Reaction and Isotopologues. *J. Phys. Chem. A* **2013**, *117*, 2678−2686.
(46) Truhlar, D. G.; Garrett, B. C. Resonance State Approach to Quantum Mechanical Variational Transition State Theory. *J. Phys. Chem.* **1992**, *96*, 6515−6518.
(47) Truhlar, D. G.; Garrett, B. C.; Klippenstein, S. J. Current Status of Transition-State Theory. *J. Phys. Chem.* **1996**, *100*, 12771−12800.
(48) Miller, W. H. Semi-Classical Theory for Non-separable Systems: Construction of "Good" Action-Angle Variables for Reaction Rate Constants. *Faraday Discuss Chem. Soc.* **1977**, *62*, 40−46.
(49) Beyer, T.; Swinehart, D. F. Number of Multiply-Restricted Partitions. *Commun. Assoc. Comput. Machines* **1973**, *16*, 379−379.
(50) Stein, S. E.; Rabinovitch, B. S. Accurate Evaluation of Internal Energy-Level Sums and Densities Including Anharmonic Oscillators and Hindered Rotors. *J. Chem. Phys.* **1973**, *58*, 2438−2445.
(51) Hu, X.; Hase, W. L.; Pirraglia, T. Vectorization of the General Monte Carlo Classical Trajectory Program Venus. *J. Comput. Chem.* **1991**, *12*, 1014−1024.
(52) Hase, W. L.; Duchovic, R. J.; Hu, X.; Komornicki, A.; Lim, K. F.; Lu, D.-H.; Peslherbe, G. H.; Swamy, K. N.; Linde, S. R. V.; Varandas, A.; et al. Venus96: A General Chemical Dynamics Computer Program. *Quantum Chem. Program Exch. Bull.* **1996**, *16*, 671.
(53) Ruscic, B.; Pinzon, R. E.; Morton, M. L.; von Laszevski, G.; Bittner, S. J.; Nijsure, S. G.; Amin, K. A.; Minkoff, M.; Wagner, A. F. Introduction to Active Thermochemical Tables: Several "Key" Enthalpies of Formation Revisited. *J. Phys. Chem. A* **2004**, *108*, 9979−9997.
(54) Ruscic, B.; Pinzon, R. E.; von Laszevski, G.; Kodeboyina, D.; Burcat, A.; Leahy, D.; Montoya, D.; Wagner, A. F. Active Thermochemical Tables: Thermochemistry for the 21st Century. *J. Phys. Conf. Ser.* **2005**, *16*, 561−570.
(55) Ruscic, B.; Pinzon, R. E.; Morton, M. L.; Srinivasan, N. K.; Su, M.-C.; Sutherland, J. W.; Michael, J. V. Active Thermochemical Tables: Accurate Enthalpy of Formation of Hydroperoxyl Radical, HO_2. *J. Phys. Chem. A* **2006**, *110*, 6592−6601.
(56) Czakó, G.; Shepler, B. C.; Braams, B. J.; Bowman, J. M. Accurate Ab Initio Potential Energy Surface, Dynamics, and Thermochemistry of the F+CH_4 → HF+CH_3 Reaction. *J. Chem. Phys.* **2009**, *130*, 084301.
(57) Li, J.; Dawes, R.; Guo, H. Kinetic and Dynamic Studies of the Cl(^2P_u) + H_2O($\tilde{X}^1A_1$) → HCL($\tilde{X}^1\Sigma^+$) + OH($\tilde{X}^2\Pi$) Reaction on an *Ab Initio* Based Full-Dimensional Global Potential Energy Surface of the Ground Electronic State of ClH_2O. *J. Chem. Phys.* **2013**, *139*, 074302.
(58) Brown, F. B.; Truhlar, D. G. A New Semi-Empirical Method of Correcting Large-Scale Configuration Interaction Calculations for Incomplete Dynamic Correlation of Electrons. *Chem. Phys. Lett.* **1985**, *117*, 307−313.
(59) Ramachandran, B.; Peterson, K. A. Potential Energy Surfaces for the ^{3}A″ and ^{3}A′ Electronic States of the O(^{3}P)+HCl System. *J. Chem. Phys.* **2003**, *119*, 9590−9600.